Structure, Spectroscopy, and Reactivity Properties of Porphyrin Pincers: A Conceptual Density Functional Theory and Time-Dependent Density Functional Theory Study

Ying Huang,[†,‡] Aiguo Zhong,[§] Chunying Rong,[†] Xiaoming Xiao,*[,†] and Shubin Liu*[,†,||]

College of Chemistry and Chemical Engineering, Hunan Normal University, Changsha, Hunan 410081, People's Republic of China, School of Pharmacy, Hunan University of Traditional Chinese Medicine, Changsha, Hunan 410007, People's Republic of China, Department of Chemistry, Taizhou College, Linhai, Zhejiang 317000, People's Republic of China, and Renaissance Computing Institute, University of North Carolina, Chapel Hill, North Carolina 27599-3455

Received: September 6, 2007; In Final Form: November 1, 2007

Porphyrin and pincer complexes are both important categories of compounds in biological and catalytic systems. The idea to combine them is computationally investigated in this work. By employment of density functional theory (DFT), conceptual DFT, and time-dependent DFT approaches, structure, spectroscopy, and reactivity properties of porphyrin pincers are systematically studied for a selection of divalent metal ions. We found that the porphyrin pincers are structurally and spectroscopically different from their precursors and are more reactive in electrophilic and nucleophilic reactions. A few quantitative linear/exponential relationships have been discovered between bonding interactions, charge distributions, and DFT chemical reactivity indices. These results are implicative in chemical modification of hemoproteins and understanding chemical reactivity in heme-containing and other biologically important complexes and cofactors.

1. Introduction

Porphyrin, a hetero- and macrocyclic compound derived from four interconnected, coplanar pyrrole-like subunits,[1,2] is the fundamental building block of hemoproteins abundant in nature and responsible for a variety of physiological functions such as storage and transportation of oxygen (hemoglobin and myoglobin), catalysis of H_2O_2 dismutation (catalase), electron transfer (e.g., cytochrome *c* and cytochrome *b*5), and oxidation of substrates (e.g., horseradish peroxidase and cytochrome P450).[1,2] The porphyrin ring in the common dianonic form has 26 π electrons and forms a highly conjugated, aromatic structure with unique properties in stability, ligand binding, spectroscopy, redox potential, etc. Chemical modifications to fathom and harness the extraordinary structural and electronic properties of this compound have been of great interests in the literature,[3−7] among which one recent example is called porphyrin pincers.

The pincer complex (see Scheme 1), first synthesized by Moulton and Shaw[8] in 1976, consists of a metallic center and a pincerlike ligand containing donor atoms in coordination in the tridentate manner with the metal ion.[9,10] The tridentate σ-bonded nature between the pincer ligand and the metal atom strongly supports the metallic center, preventing it from dissociation and thus achieving high thermal stability. Meanwhile, choices of donor atoms allow the fine tuning of the steric and electronic properties of the pincer complexes. Common tridentate atoms include NCN,[11] OCO,[12] PCP,[13] SCS,[14] SPS,[15] etc. The pincer complex often exhibits pronounced structure, spectroscopy, and reactivity properties different from its precursor, leading to its profuse applications in different areas of chemistry, particularly in catalysis.

SCHEME 1

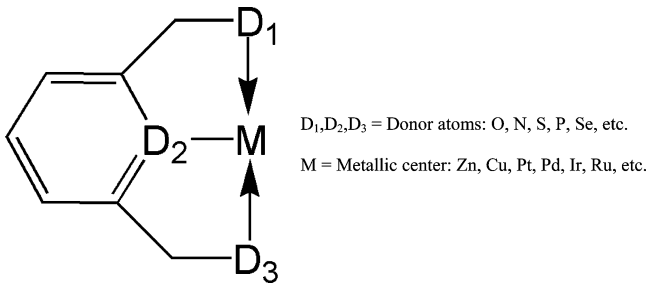

More recently, the idea of combining porphyrin with the pincer complex has been explored.[16−20] This idea is appealing in that porphyrin employs the inner cavity to form peripherally metalated complex with one divalent metal ion, whereas a second, more often different, metal ion utilizes side donor atoms of the macrocycle to form the pincer complex. This modification of the porphyrin is relevant because heme motifs in hemoproteins have two carboxylate "arms", which can serve as electron donors and are implicative in physiological functions. It is anticipated and has been demonstrated that because of the coupling between the two metal ions this heterobimetallic complex offers distinctive physiochemical properties such as magnetism, photochemistry, and reactivity in metal-catalyzed reactions from its precursors.[20]

In this work, we employ quantum mechanical computational tools from density functional theory (DFT),[21] conceptual DFT,[22] and time-dependent DFT (TD-DFT)[23−27] to investigate the structural, spectroscopic, and reactivity properties of this category of complexes and compare them with those of the precursor. We found that porphyrin pincers are structurally distinctive and chemically more reactive, confirming experi-

* To whom correspondence should be addressed; E-mail: xmxiao@hunnu.edu.cn (X.M.X.); shubin@email.unc.edu (S.B.L.).
† Hunan Normal University.
‡ Hunan University of Traditional Chinese Medicine.
§ Taizhou College.
|| University of North Carolina.

10.1021/jp077178t CCC: $40.75
Published on Web 12/20/2007

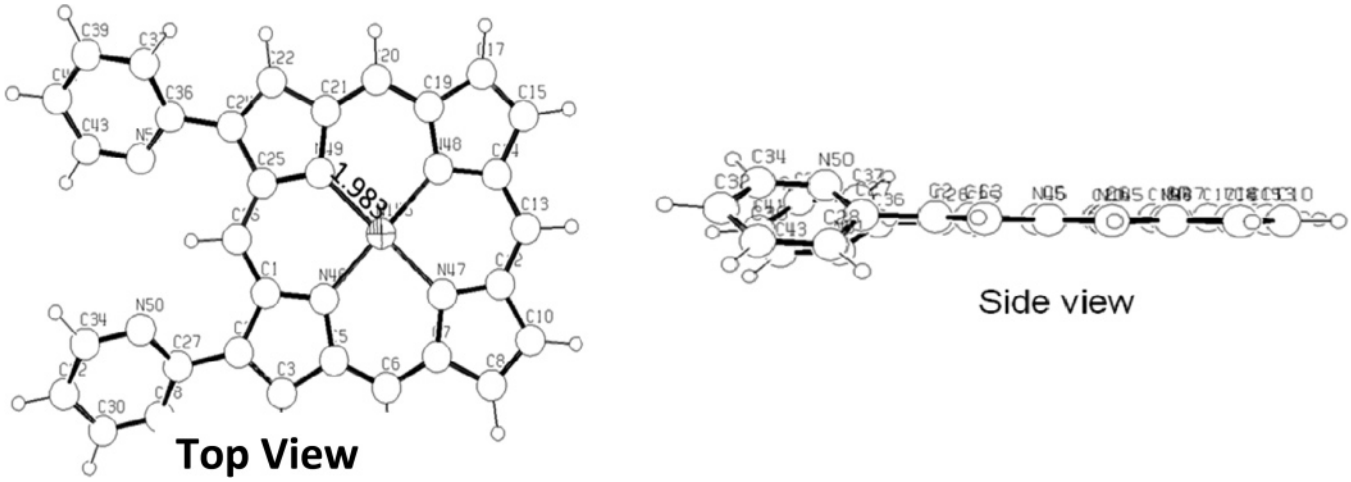

Figure 1. Top and side views of the optimized structure of 2M (M = H, Mg, Fe, Ni, Cu, and Zn).

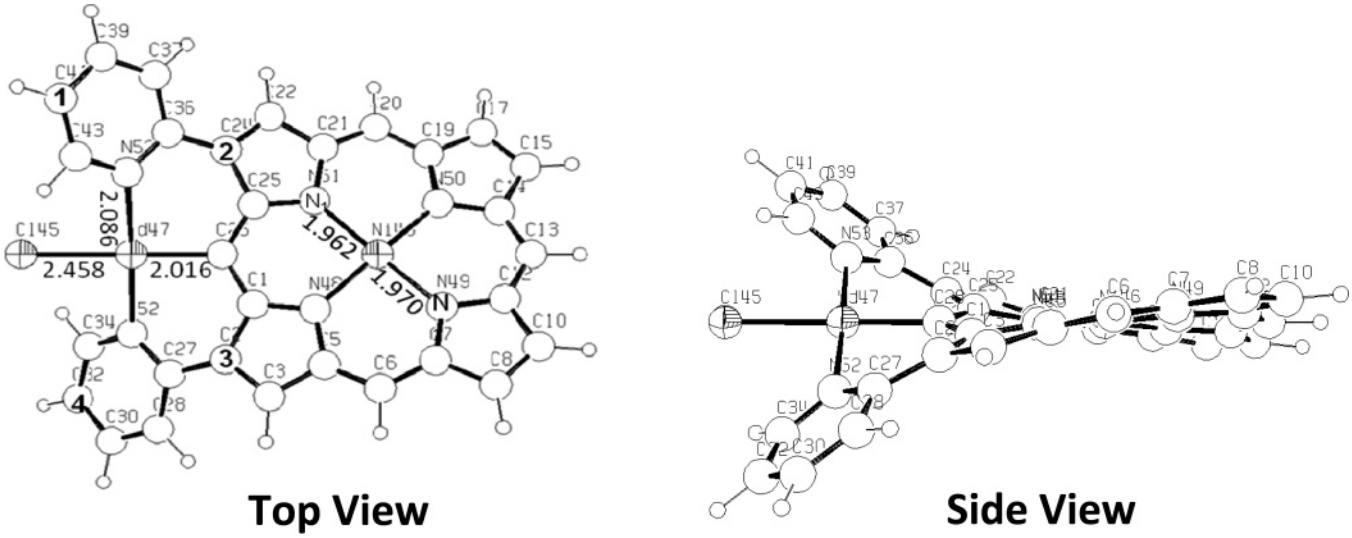

Figure 2. Top and side views of the optimized structure of 3M (M = H, Mg, Fe, Ni, Cu, and Zn).

SCHEME 2

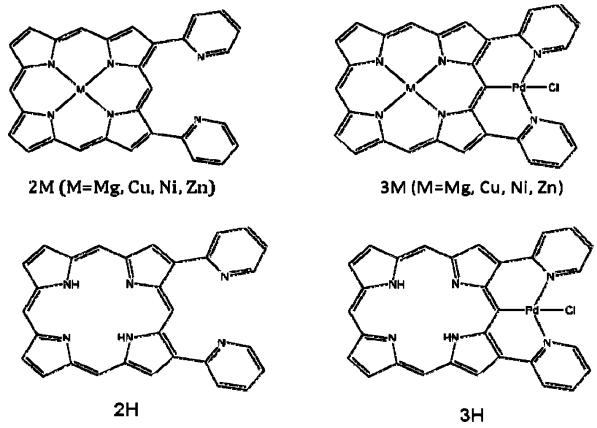

mental findings and suggesting that they can serve as valuable substitutes in chemical modification of porphyrin in hemoproteins.

II. Computational Methodology

Scheme 2 shows the systems that we have studied in this work, where porphyrin pincers are denoted by 3M (M = H, Mg, Fe, Ni, Cu, and Zn) with the corresponding precursor by 2M (M = H, Mg, Fe, Ni, Cu, and Zn), and in all cases, the second metal cation is divalent Pd. Structurally speaking, as shown in Scheme 2, 2H and 3H are different from others because they do not have the first metalation in the porphyrin inner cavity.

All calculations were performed with the B3LYP[28−30] functional and a generic basis set, where C and H use Pople's valence-split double-ζ 6-31G basis set and the electronegative N and first metal element employ the 6-311+G(d) basis set.[31,32] This generic basis set[33−35] has been shown to be effective, both efficient and reliable, in predicting structural and reactivity properties for hemelike systems.[36] For Pd, we use the ECP Stuggart basis set.[37] Structural optimization was performed for both 2M and 3M systems at first, and then a frequency calculation was carried out to check that the optimized structure is indeed a minimum (with no imaginary frequency). A natural bond orbital (NBO) analysis[38] is conducted to obtain the condensed natural orbital charge distribution of the systems and to perform the second-order perturbation theory analysis of the Fock matrix in NBO basis to obtain the porphyrin−metal and pincer−metal interaction energies. TD-DFT calculations are followed to obtain their UV/vis spectra. As we noticed earlier, spin multiplicity[39−41] is an important issue for transition metals, for M = Fe, Ni, and Cu, different spin states are possible. Our studies show that for each of them in both 2M and 3M complexes the lowest spin state ($S = {}^1/_2$ for Cu and $S = 0$ for

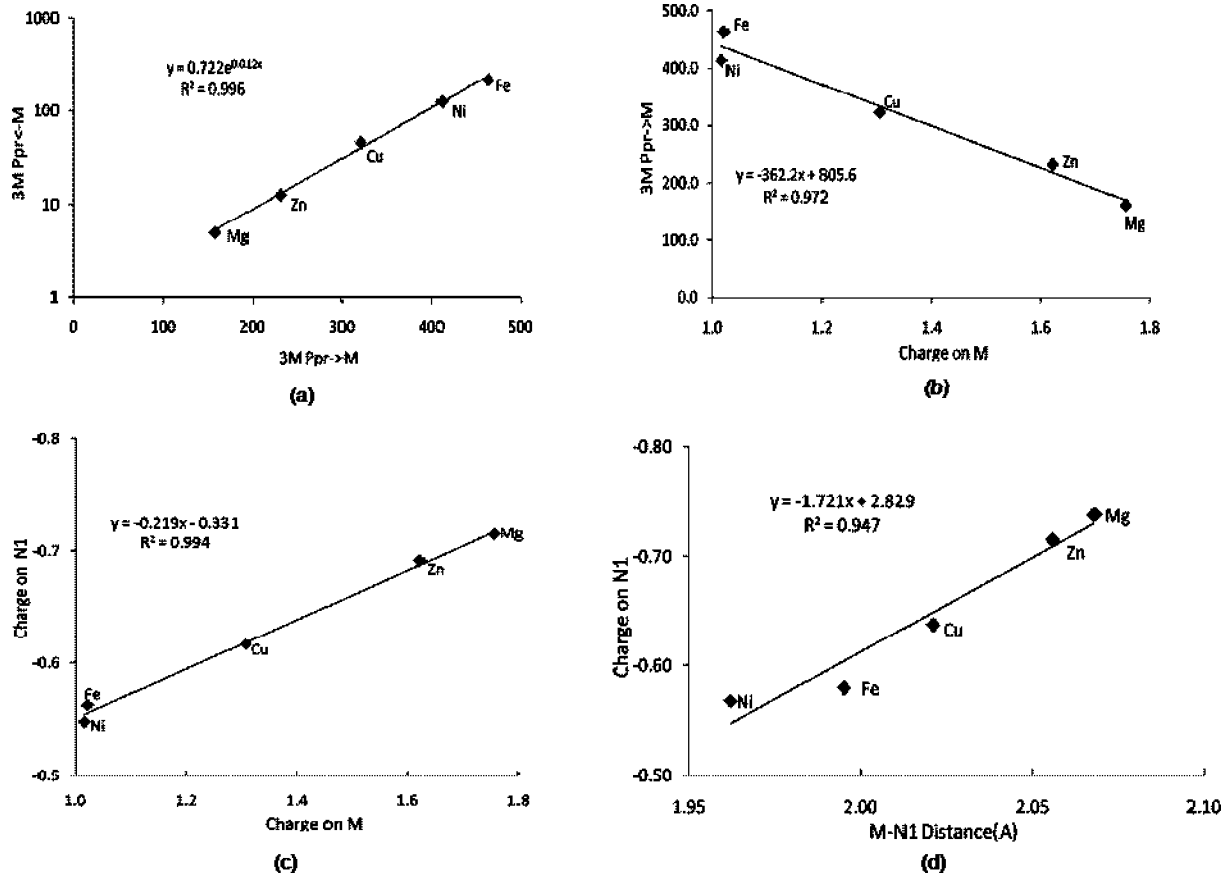

Figure 3. Quantitative relationships stemming from the NBO and second-order perturbation theory analyses for 2M and 3M systems.

TABLE 1: Selected Parameters from the Optimized Structure for 2M and 3M Systems

	3H	2Mg	3Mg	2Fe	3Fe	2Ni	3Ni	2Cu	3Cu	2Zn	3Zn
M−N_1		2.069	2.068	2.011	1.995	1.983	1.962	2.028	2.021	2.059	2.056
M−N_2		2.070	2.069	2.011	2.004	1.983	1.970	2.029	2.023	2.060	2.052
Pd−C	2.013		2.017		2.018		2.016		2.017		2.018
Pd−N	2.092		2.087		2.086		2.086		2.086		2.087
Pd−Cl	2.452		2.464		2.461		2.458		2.461		2.463
∠M−Pd−Cl			179.9		180.0		180.0		179.9		180.0
∠C1−C2−C3−C4	63.2	3.6	61.8	4.3	64.4	4.6	65.1	4.0	64.7	3.6	64.5

TABLE 2: NBO Charge and Second-Order Perturbation Theory Analyses of Porphyrin−Metal and Pincer−Metal Interactions for 2M and 3M Systems

	NBO charges				second-order PT analysis (kcal/mol)[a]			
	M	N_1	N_2	Pd	Ppr → M	Ppr ← M	Pnc → Pd	Pnc ←Pd
2H		−0.532	−0.568					
3H		−0.524	−0.572	0.657			256.6	383.9
2Mg	1.755	−0.722	−0.734		150.3	85.7		
3Mg	1.756	−0.715	−0.738	0.654	161.2	5.0	252.7	1005.5
2Fe	1.232	−0.592	−0.604		393.9	63.3		
3Fe	1.021	−0.563	−0.580	0.653	463.2	217.5	225.8	427.1
2Ni	1.022	−0.555	−0.567		391.2	111.2		
3Ni	1.016	−0.548	−0.568	0.654	413.8	126.6	251.6	387.1
2Cu	1.308	−0.624	−0.635		291.8	40.5		
3Cu	1.306	−0.617	−0.637	0.654	322.4	45.7	248.5	392.3
2Zn	1.620	−0.699	−0.710		228.8	60.7		
3Zn	1.622	−0.691	−0.715	0.654	232.9	12.7	256.7	1009.9

[a] Ppr → M stands for the donor−acceptor interaction between Ppr (porphyrin) and M (metal), and Ppr serves as the electron donor and M as the electron acceptor. Pnc → Pd denotes the donor−acceptor interaction between Pnc (pincer) and M (metal), and Pnc serves as the electron donor and M as the electron acceptor. The total interaction, in kcal/mol, is the sum of all orbital contributions larger than 0.05 kcal/mol.

Fe and Ni) possesses the lowest energy. We employ the lowest spin state for each system in the present study.

DFT reactivity indices are conceptually insightful and practically convenient in predicting chemical reactivity and regioselectivity of a molecule. In DFT,[21] the chemical potential, μ, and hardness, η, are defined as $\mu = -\chi = (\partial E/\partial N)_v$ and $\eta = (\partial^2 E/\partial N^2)_v = (\partial \mu/\partial N)_v$, where E is the total energy of the system, N is the number of electrons in the system, and v is the external potential. The chemical potential μ can be identified as the negative of electronegativity (χ).[42] According to Mulliken,[43] one

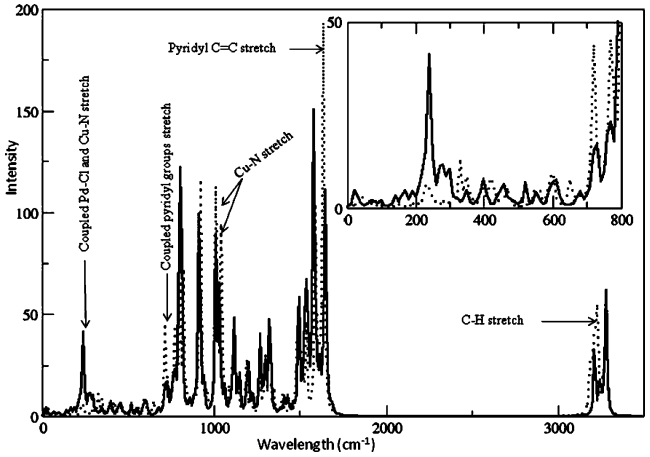

Figure 4. Comparison of calculated IR spectra between 2Cu (dotted line) and 3Cu (solid line) systems.

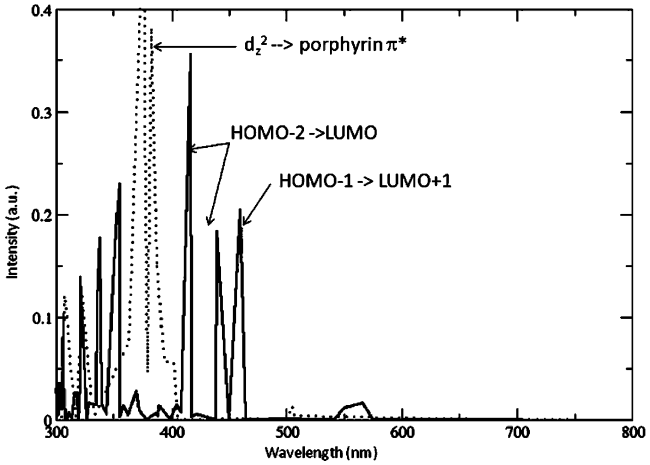

Figure 5. Comparison of calculated UV/vis spectra between 2Ni (dotted line) and 3Ni (solid line) systems using the TD-DFT method.

has $\mu = -\chi = -(1/2)(I + A)$ and $\eta = I - A$,[44] where I and A are the first ionization potential and electron affinity, respectively. Under the Koopmans' theorem for closed-shell molecules, based on the finite difference approach, I and A can be expressed in terms of the highest occupied molecular orbital (HOMO) energy, ϵ_{HOMO}, and the lowest unoccupied molecular orbital (LUMO) energy, ϵ_{LUMO}, respectively, $I \approx -\epsilon_{HOMO}$; $A \approx -\epsilon_{LUMO}$. Recently, Parr, Szentpaly, and Liu[45] introduced the concept of electrophilicity index, ω, in terms of μ and η, $\omega = \mu^2/2\eta$, appraising the capacity of an electrophile to accept the maximal number of electrons in a neighboring reservoir of electron sea. More recently, Ayers and co-workers[46−48] have proposed two new reactivity indices to quantify nucleophilic and electrophilic capabilities of a leaving group, nucleofugality $\Delta E_n \equiv -A + \omega = (\mu + \eta)^2/2\eta$ and electrofugality $\Delta E_e \equiv I + \omega = (\mu - \eta)^2/2\eta$. These reactivity indices from the conceptual DFT framewoek, μ, η, ω, ΔE_n, and ΔE_e, are used to appraise the chemical reactivity of both 2M and 3M systems. All calculations are performed with the Gaussian 03 package[49] with tight self-consistent field convergence and ultrafine integration grids.

III. Results and Discussion

Table 1 shows a few selected bond distances and angles from the optimized structure of 2M and 3M systems. One finds that there exists little change in Pd−C, Pd−N, and Pd−Cl bond lengths as well as the M−Pd−Cl angle among different divalent 3M systems when a metal ion is in the inner cavity of porphyrin. For Mg where there is no 3d electron, the bond length of Mg−N_1 and Mg−N_2 between 2M and 3M systems is almost the same, only by a change of 0.001 Å. For transition metals, M−N_1 and M−N_2 are shortened after the pincer complex is formed because of the backbonding interactions between the pincer donor atoms and Pd cation. For example, Fe−N_1 distance changes to 1.995 from 2.011 Å. The main difference between 2M and 3M structures, however, lies in the ∠C1−C2−C3−C4 dihedral angle, where one observes a substantial change from ∼5° in 2M to ∼65° in 3M. This change is needed to bring the donor atoms together to form the pincer complex. Figures 1 and 2 illustrate the structure difference between 2M (Figure 1, two views) and 3M (Figure 2, two views) systems, where it is seen that, before the pincer complex is formed (Figure 1), all atoms in the porphyrin macrocycle ring stay in the same plane, whereas after the pincer complex is formed, shown in Figure 2, the plane becomes twisted with the two pyridyl groups pointing away and lying in the different side of the porphyrin ring.

Table 2 shows the charge distribution for a selected list of atoms from the NBO analysis and the donor−acceptor interaction energies from the second-order perturbation theory in NBO bases. It is seen from Table 2 that the positive charge on Pd is almost unchanged, 0.654, across different metals. Mg has the largest positive charge, and its accompanying N_1/N_2 atoms are most negative, indicating that Mg−N_1 and Mg−N_2 bonds are most ionic within the series. On the other hand, Ni is least charged in the series, and thus the Ni−N_1 and Ni−N_2 bonds are of the covalent nature. In the donor−acceptor back-bonding interactions, it is observed that except for the Fe system where a little smaller value is found, the pincer (as donor) → Pd (as acceptor) interaction is more or less a constant, ∼250 kcal/mol. For other parts of the interaction, such as porphyrin (donor) → M (acceptor), M (donor) → porphyrin (acceptor), and Pd (donor) → pincer (acceptor), large variance in the magnitude of the interaction has been discovered. Since Mg does not have d orbital electrons and Zn's d shell is full, it is expected that their M → porphyrin interaction is small, as confirmed by the data, 5.0 and 12.7 kcal/mol, respectively, from Table 2. The metal cation that possesses the strongest donor−acceptor interaction with the porphyrin ring is iron, whose porphyrin → Fe and Fe → porphyrin energies are 463.2 and 217.5 kcal/mol, respectively. These strong back-bonding interactions between Fe and the macrocyle, which as a result may keep the scaffold both stable and reactive, might be an important reason that nature chooses iron as an integral ingredient of hemoproteins to perform redox and other life-essential processes. We notice also that even though the pincer → Pd interaction is approximately constant, the reverse interaction is not. For example, with no metal ion in the inner cavity of porphyrin, in 3H, the Pd → pincer energy is 383.9 kcal/mol, but it becomes 427.1 kcal/mol in 3Fe, 1005.5 kcal/mol in 3Mg, and 1009.9 kcal/mol in 3Zn. This drastic variation in the backbonding flow of electrons from Pd to the pincer's unoccupied π^* orbitals in different 3M systems is an indication of the dependence of the electron distribution of the macrocycle ring on the first metal ion, M, in the porphyrin inner cavity. Because there exists strong donor−acceptor interactions between transition-metal ion M in the inner cavity and the porphyrin ring, d-electron donations of the second metal ion, Pd, to the π^* orbitals of porphyrin are hindered, leading to the smaller Pd → pincer interaction. On the other hand, for 3Mg and 3Zn systems, where either there is no d-electron or the

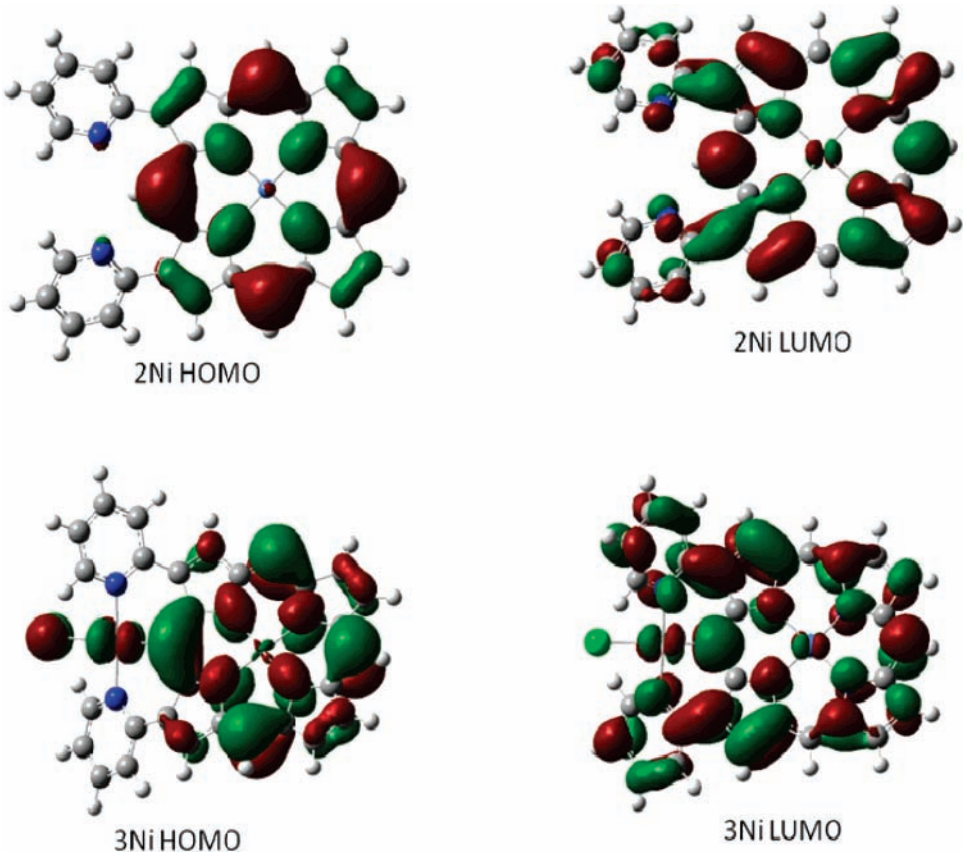

Figure 6. Comparison of HOMO and LUMO orbitals for 2Ni and 3Ni systems.

TABLE 3: Calculated DFT Reactivity Indices for 2M and 3M Systems (Units in au)

	HOMO	LUMO	μ	η	ω	ΔE_n	ΔE_e
2H	−0.186	−0.085	0.135	0.051	0.181	0.342	0.071
3H	−0.187	−0.098	0.142	0.045	0.227	0.392	0.107
2Mg	−0.186	−0.082	0.134	0.052	0.172	0.332	0.064
3Mg	−0.187	−0.095	0.141	0.046	0.217	0.381	0.099
2Fe	−0.190	−0.100	0.144	0.045	0.233	0.400	0.111
3Fe	−0.191	−0.107	0.149	0.042	0.264	0.434	0.136
2Ni	−0.191	−0.080	0.136	0.056	0.165	0.328	0.057
3Ni	−0.192	−0.094	0.143	0.049	0.207	0.375	0.089
2Cu	−0.190	−0.081	0.136	0.054	0.170	0.333	0.061
3Cu	−0.190	−0.095	0.143	0.048	0.213	0.380	0.095
2Zn	−0.189	−0.082	0.135	0.054	0.171	0.333	0.062
3Zn	−0.189	−0.095	0.142	0.047	0.214	0.380	0.096

d-shell is full for the metal cation M in the inner cavity of the porphyrin ring, the back-bonding interaction between M and porphyrin is weaker, and thus the virtual orbitals of the conjugate macrocyclic ring are less disturbed, leading to stronger interactions with the second metal ion, Pd, in the pincer complex.

Shown in Figure 3 are a few quantitative relationships obtained from the NBO and second-order perturbation theory analyses for 3M systems. In Figure 3a, we found that back-bonding interactions between porphyrin → M and M → porphyrin follow an exponential relationship with a positive exponent, indicating that the larger the porphyrin → M interaction, the larger the M → porphyrin interaction. In parts b−d of Figure 3, linear relationships are observed between the porphyrin → M interaction and charge on M (Figure 3b), between charges on M and N_1 (Figure 3c), and charge on N_1 and distance of M−N_1 (Figure 3d) with a negative slope in Figure 3b and positive one in others, demonstrating that the larger the porphyrin→M interaction, the less the charge on M (more of covalent nature) (Figure 3b), the more the charge on N_1, the more charge on M (Figure 3c), and the longer the M−N_1 bond (Figure 3d).

We also calculated the IR/Raman spectra for all 2M and 3M systems. Shown in Figure 4 as an example is the comparison of the IR spectra between 2Cu (dotted line) and 3Cu (solid line) systems. The peaks have been broadened by fitting to a Gaussian function. It is seen from Figure 4 that, because of the formation of the pincer complex, some peaks such as those associated with the coupled pyridyl groups and C═C stretches become weaker, whereas in other regions one observes new peaks in 3M (see the insertion of the Figure) or peaks that become stronger after the pincer complex is formed.

Recent experimental evidence[20] suggests that the UV/vis spectra of the porphyrin pincers exhibit different absorption spectra from their precursors with the first peak significantly red-shifted. To ascertain the origin of such differences we performed TD-DFT[23−27] calculations at the B3LYP/6-311+G* level. Figure 5 displays the comparison of the UV/vis spectra between 2Ni (dotted line) and 3Ni (solid line) systems. In accordance with the experiments, we found that, compared to those of 2Ni, 3Ni's absorption peaks are indeed significantly red-shifted, but because of the difference in their molecular structures, the nature of the transitions associated with each peak is also different. For example, the peaks near 360 nm in 2Ni are transitions from Ni's $3d_{z^2}$ to porphyrin π^* molecular orbital, but in 3M, the red-shifted peaks are associated with transitions from orbitals close to HOMO and LUMO, which are shown in Figure 6. From the Figure, it is observed that the HOMO electron distribution in both the 2Ni and 3Ni systems is similar, and noticeable differences between the two systems come from the LUMO, especially in the two pyridyl groups.

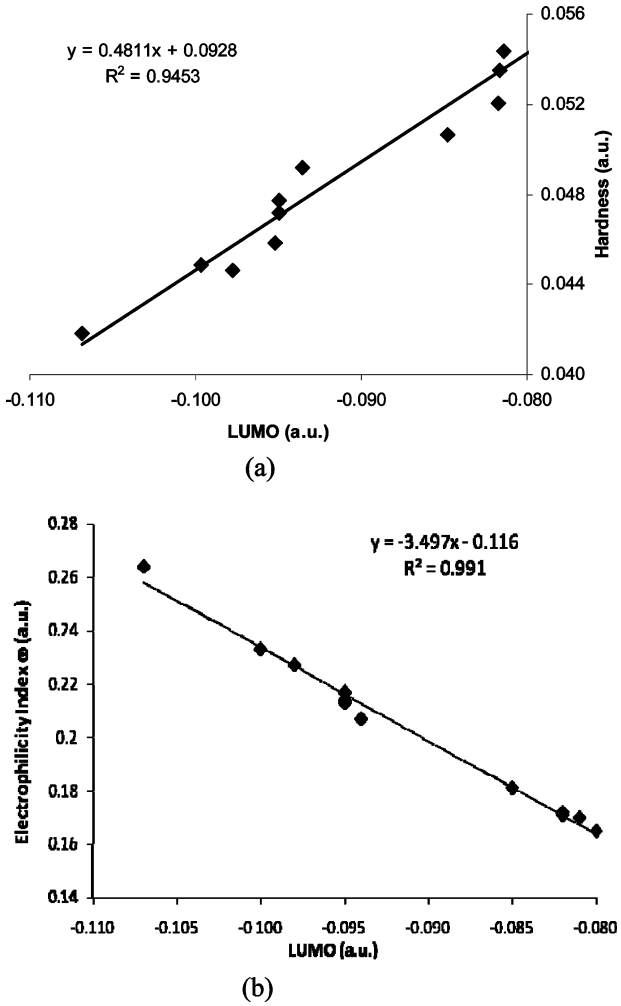

Figure 7. Linear relationships obtained from DFT reactivity indices of the 2M and 3M systems: (a) LUMO vs hardness and (b) LUMO vs electrophilicity index.

To understand the reactivity difference between the porphyrin pincer complex and its precursor, we employ conceptual DFT reactivity indices. Shown in Table 3 are their numerical data from HOMO and LUMO. It is observed that between each pair of 2M and 3M (M = H, Mg, Fe, Ni, Cu, and Zn) systems: (i) the HOMO does not change noticeably, and it is the LUMO that contributes the majority of the difference to the HOMO−LUMO gap between 2M and 3M; and (ii) for each pair, compared to 2M, we find that 3M's global hardness is always smaller (less stable and thus more reactive), and electrophilicity ω, electrofugality ΔE_e, and nucleofugality ΔE_n indices are always larger, confirming that 3M is indeed more reactive than 2M. To verify that the reactivity difference between 2M and 3M mainly comes from the LUMO, shown in Figure 7, are the relationships between the LUMO energy and hardness (Figure 7a) and between LUMO and electrophilicity index ω (Figure 7b), where a good linear relationship between the two quantities with the correlation coefficient $R^2 > 0.9$ in each of the cases is observed. Notice that the correlation between LUMO, which is a reasonable estimation of the electron affinity, and the electrophilicity index shown in Figure 7b has been observed earlier.[45]

IV. Conclusions

The idea of combining porphyrin ring with pincer complex is computationally explored in this work for a series of systems (2M and 3M, where M = H, Mg, Fe, Ni, Cu, and Zn), whose structure, spectroscopy, and reactivity properties are systematically investigated by DFT, conceptual DFT, and TD-DFT approaches. In accordance with earlier experiments, we found that, in comparison with 2M, 3M is structurally and spectroscopically different from and more reactive than its precursor. We also found that the reactivity difference mainly comes from the LUMO. In addition, a few linear/exponential relationships have been discovered in binding interactions, charge distributions, and DFT chemical reactivity indices of the systems concerned. The results from the present work might have implications in chemical modification of hemoproteins and in understanding chemical reactivity difference in heme-containing and other metal-containing biologically important complexes and cofactors.

Acknowledgment. We thank the Virtual Laboratory for Computational Chemistry, Computer Network Information Center, Chinese Academy of Sciences, for allowing us to access its computing facilities for the present study.

References and Notes

(1) Denisov, I. G.; Makris, T. M.; Sligar, S. G.; Schlichting, I. *Chem. Rev.* **2005**, *105*, 2253.
(2) Shaik, S.; Kumar, D.; de Visser, S. P.; Altun, A.; Thiel, W. *Chem. Rev.* **2005**, *105*, 2279.
(3) Ma, L. H.; Liu, Y.; Zhang, X.; Yoshida, T.; Langry, K. C.; Smith, K. M.; La Mar, G. N. *J. Am. Chem. Soc.* **2006**, *128*, 6391.
(4) Sasaki, M.; Shibano, Y.; Tsuji, H.; Araki, Y.; Tamao, K.; Ito, O. *J. Phys. Chem. A* **2007**, *111*, 2973.
(5) Xenogiannopoulou, E.; Medved, M.; Iliopoulos, K.; Couris, S.; Papadopoulos, M. G.; Bonifazi, D.; Sooambar, C.; Mateo-Alonso, A.; Prato, M. *Chem. Phys. Chem.* **2007**, *8*, 1056.
(6) Kadish, K. M.; Wenbo, E.; Zhan, R. Q.; Khoury, T.; Govenlock, L. J.; Prashar, J. K.; Sintic, P. J.; Ohkubo, K.; Fukuzumi, S.; Crossley, M. J. *J. Am. Chem. Soc.* **2007**, *129*, 6576.
(7) Durr, K.; Macpherson, B. P.; Warratz, R.; Hampel, F.; Tuczek, F.; Helmreich, M.; Jux, N.; Ivanovic-Burmazovic, I. *J. Am. Chem. Soc.* **2007**, *129*, 4217.
(8) Moulton, C. J.; Shaw, B. L. *J. Chem. Soc., Dalton Trans.* **1976**, 1020.
(9) Peris, E.; Crabtree, R. H. *Coord. Chem. Rev.* **2004**, *248*, 2239.
(10) van der Boom, M. E.; Misltein, D. *Chem. Rev.* **2003**, *103*, 1759−1792.
(11) Ma, L.; Imbesi, P. M.; Updegraff, J. B.; Hunter, A. D.; Protasiewicz, J. D. *Inorg. Chem.* **2007**, *46*, 5220.
(12) Stol, M.; Snelders, D. J. M.; de Pater, J. J. M.; van Klink, G. P. M.; Kooijman, H.; Spek, L, A.; van Koten, G. *Organometallics* **2005**, *24*, 743.
(13) Ozerov, O. V.; Watson, L. A.; Pink, M.; Caulton, K. G. *J. Am. Chem. Soc.* **2007**, *129*, 6003.
(14) Okamoto, K.; Kanbara, T.; Yamamoto, T.; Wada, A. *Organometallics* **2006**, *25*, 4026.
(15) Arliguie, T.; Doux, M.; Mezailles, N.; Thuery, P.; Le Floch, P.; Ephritikhine, M. *Inorg. Chem.* **2006**, *45*, 9907.
(16) Huck, W. T. S.; Rohrer, A.; Anikumar, A. T.; Fokkens, R. H.; Nibbering, N. M. M.; van Veggel, F. C. J. M.; Reinhoudt, D. N. *New J. Chem.* **1998**, 165.
(17) Dixon, I. M.; Collin, J. P. *J. Porphyrins Phthalocyanines* **2001**, *5*, 600.
(18) Suijkerbuijk, B. M. J. M.; Lutz, M.; Spek, A. L.; van Koten, G.; Klein Gebbink, R. J. M. *Org. Lett.* **2004**, *6*, 3023.
(19) Hata, H.; Shinokubo, H.; Osuka, A. *J. Am. Chem. Soc.* **2005**, *127*, 8264.
(20) Yamaguchi, S.; Katoh, T.; Shinokubo, H.; Osuka, A. *J. Am. Chem. Soc.* **2007**, *129*, 6392.
(21) Parr, R. G.; Yang, W. *Density Functional Theory of Atoms and Molecules*; Oxford University Press: Oxford, 1989.
(22) Geerlings, P.; De Proft, F.; Langenaeker, W. *Chem. Rev.* **2003**, *103*, 1793.
(23) Runge, E.; Gross, E. K. U. *Phys. Rev. Lett.* **1984**, *52*, 997.
(24) Stratmann, R. E.; Scuseria, G. E.; Frisch, M. J. *J. Chem. Phys.* **1998**, *109*, 8218.
(25) Marques, M. A. L.; Gross, E. K. U. *Annu. Rev. Phys. Chem.* **2004**, *55*, 427.
(26) Furche, F.; Rapport, D. *Comput. Theor. Chem* **2005**, *16*, 93.

(27) Dreuw, A.; Head-Gordon, M. *Chem. Rev.* **2006**, *105*, 4009.
(28) Becke, A. D. *Phys. Rev. A* **1988**, *38*, 3098.
(29) Becke, A. D. *J. Chem. Phys.* **1993**, *98*, 5648.
(30) Lee, C.; Yang, W.; Parr, R. G. *Phys. Rev. B* **1988**, *37*, 785.
(31) Krishnan, R.; Binkley, J. S.; Seeger, R.; Pople, J. A. *J. Chem. Phys.* **1980**, *72*, 650.
(32) Frisch, M. J.; Pople, J. A.; Binkley, J. S. *J. Chem. Phys.* **1984**, *80*, 3265.
(33) Zhang, R. Q.; Lifshitz, C. *J. Phys. Chem.* **1996**, *100*, 960.
(34) Zhang, R. Q.; Huang, J. H.; Bu, Y. X.; Han, K. L.; Lee, S. T.; He, G. Z. *Science in China (Series B*) **2000**, *43*, 375.
(35) Fan, W. J.; Zhang, R. Q.; Liu, S. B. *J. Comput. Chem.* **2007**, *28*, 967.
(36) Rong, C.; Lian, S. X.; Yin, D. L.; Zhong, A. G.; Zhang, R. Q.; Liu, S. B. *Chem. Phys. Lett.* **2007**, *434*, 149.
(37) Dolg, M.; Stoll, H.; Preuss, H.; Pitzer, R. M. *J. Phys. Chem.* **1993**, *97*, 5852.
(38) Reed, A. E.; Curtiss, L. A.; Weinhold, F. *Chem. Rev.* **1988**, *88*, 899.
(39) Liu, S. B.; Langenaeker, W. *Theor. Chem. Acc.* **2003**, *110*, 338.
(40) Zhong, A. G.; Liu, S. B. *J. Theory Comput. Chem.* **2005**, *4*, 833.
(41) Rong, C.; Lian, S.; Yin, D.; Shen, B.; Zhong, A. G.; Bartolotti, L.; Liu, S. B. *J. Chem. Phys.* **2006**, *125*, 174102.
(42) Iczkowski, R. P.; Margrave, J. L. *J. Am. Chem. Soc.* **1961**, *83*, 3547.
(43) Mulliken, R. S. *J. Chem. Phys.* **1934**, *2*, 782.
(44) Ayers, P. W.; Parr, R. G.; Pearson, R. G. *J. Chem. Phys.* **2006**, *124*, 194107.
(45) Parr, R. G.; Szentpaly, L. V.; Liu, S. B. *J. Am. Chem. Soc.* **1999**, *105*, 1922.
(46) Ayers, P. W.; Anderson, J. S. M.; Rodriguez, J. I.; Jawed, Z. *Phys. Chem. Chem. Phys.* **2005**, *7*, 1918.
(47) Ayers, P. W.; Anderson, J. S. M.; Bartolotti, L. J. *Int. J. Quantum Chem.* **2005**, *101*, 520.
(48) Roos, G.; Loverix, S.; Brosens, E.; Van Belle, K.; Wyns, L.; Geerlings, P.; Messens, J. *Chem. Biochem.* **2006**, *7*, 981.
(49) Frisch, M. J.; Trucks, G. W.; Schlegel, H. B.; Scuseria, G. E.; Robb, M. A.; Cheeseman, J. R.; Montgomery, J. A., Jr.; Vreven, T.; Kudin, K. N.; Burant, J. C.; Millam, J. M.; Iyengar, S. S.; Tomasi, J.; Barone, V.; Mennucci, B.; Cossi, M.; Scalmani, G.; Rega, N.; Petersson, G. A.; Nakatsuji, H.; Hada, M.; Ehara, M.; Toyota, K.; Fukuda, R.; Hasegawa, J. Ishida, M.; Nakajima, T.; Honda, Y.; Kitao, O.; Nakai, H.; Klene, M.; Li, X.; Knox, J. E.; Hratchian, H. P.; Cross, J. B.; Adamo, C.; Jaramillo, J.; Gomperts, R.; Stratmann, R. E.; Yazyev, O.; Austin, A. J.; Cammi, R.; Pomelli, C.; Ochterski, J. W.; Ayala, P. Y.; Morokuma, K.; Voth, G. A.; Salvador, P.; Dannenberg, J. J.; Zakrzewski, V. G.; Dapprich, S.; Daniels, A. D.; Strain, M. C.; Farkas, O.; Malick, D. K.; Rabuck, A. D.; Raghavachari, K.; Foresman, J. B.; Ortiz, J. V.; Cui, Q.; Baboul, A. G.; Clifford, S.; Cioslowski, J.; Stefanov, B. B.; Liu, G.; Liashenko, A.; Piskorz, P.; Komaromi, I.; Martin, R. L.; Fox, D. J.; Keith, T.; Al-Laham, M. A.; Peng, C. Y.; Nanayakkara, A.; Challacombe, M.; Gill, P. M. W.; Johnson, B.; Chen, W.; Wong, M. W.; Gonzalez, C.; Pople, J. A. *Gaussian 03*, revision D.02; Gaussian, Inc.: Pittsburgh, PA, 2003.